Journal of Applied Mechanics and Technical Physics, Vol. 50, No. 3, pp. 396–405, 2009

TWO-FLUID MAGNETOHYDRODYNAMIC MODEL OF PLASMA FLOWS IN A QUASI-STEADY-STATE ACCELERATOR WITH A LONGITUDINAL MAGNETIC FIELD

A. N. Kozlov

UDC 519.6; 533.9

This paper reports the results of numerical studies of axisymmetric flows in a coaxial plasma accelerator in the presence of a longitudinal magnetic field. The calculations were performed using a two-dimensional two-fluid magnetohydrodynamic model taking into account the Hall effect and the conductivity tensor of the medium. The numerical experiments confirmed the main features of the plasmadynamic processes found previously using analytical and one-fluid models and made it possible to study plasma flows near the electrodes.

Key words: *plasma flow, magnetohydrodynamic model, Hall effect, plasma accelerator, longitudinal magnetic field.*

Introduction. In coaxial plasma accelerators [1] with azimuthal magnetic field H_φ, plasma acceleration is due to the Ampére force. The current crisis phenomenon [1, 2] prevents the attainment of high velocities in accelerators with impermeable electrodes. This phenomenon is caused by the adverse effect of the Hall effect leading to a plasma deficiency near the anode. Large-amplitude oscillations occur in the accelerator. These phenomena exert the greatest effect on the volt-ampere characteristics corresponding to a constant flow rate of matter. If the discharge current in the system is higher than a certain critical value, the discharge voltage begins to grow rapidly and the system prevents the passage of high currents. Overcoming of the current crisis is possible in two-stage systems of the type of quasi-steady-state plasma accelerators (QSPAs) [1–3]. The first stage of QSPAs consists of several small coaxial plasma accelerators for plasma ionization and its preliminary acceleration. The second stage is a large coaxial plasma accelerator connected to an independent electric circuit. Experimental studies of QSPAs have shown a high degree of stability and azimuthal symmetrization of the flows (see, for example, [4, 5]). The attained parameters values (particle concentration $n \geqslant 10^{20}$ m^{-3}, plasma velocity $V \approx 10^4$–10^6 m/sec) indicate that these accelerators are promising for use not only in developing new technologies but also in space engineering, as electrojet plasma engines, and in other areas. Modern QSPAs are designed to use ion current transport with permeable electrodes. In this regime, the electrodes are equipotential surfaces and should be permeable to plasma. The self-consistent plasma flow through the electrodes is due to the Hall effect. Ignoring this effect ($\boldsymbol{V}_e = \boldsymbol{V}_i$), the regime of impermeable continuous equipotential electrodes occurs, which is degenerate in physical practice ($\boldsymbol{V}_e \neq \boldsymbol{V}_i$). Analytical and numerical studies of processes in accelerators for a dense plasma have been performed for magnetohydrodynamic (MHD) models in the absence of a longitudinal field (see, for example, [6–8]).

The introduction of an additional longitudinal magnetic field in a plasma accelerator generates a peculiar additional channel for controlling dynamic processes in the accelerator and other devices whose operating principle is based on using the azimuthal magnetic field component. The longitudinal magnetic field causes the plasma to rotate around the axis of the system. The presence of an additional longitudinal field allows one to study the entire variety of the processes involved in the plasma flows dynamics. In practice, the introduction of a longitudinal field

Keldysh Institute of Applied Mathematics, Russian Academy of Sciences, Moscow 125047; ankoz@keldysh.ru.
Translated from Prikladnaya Mekhanika i Tekhnicheskaya Fizika, Vol. 50, No. 3, pp. 44–55, May–June, 2009. Original article submitted November 9, 2007; revision submitted February 27, 2008.

into a system involves the design of modified plasma accelerators in addition to existing QSPAs with the complex bulky system of anode transformers. Theoretical studies of two-dimensional axisymmetric steady-state flows of an ideally conducting two-component plasma in the presence of a longitudinal field [9] have been performed in an approximation of a smooth channel [1]. These studies have made it possible to reveal and analyze the major properties of plasma flows in the presence of a longitudinal magnetic field. According to the hierarchy of numerical models, as a first stage it is planned to study the plasma dynamics using a one-fluid MHD model. Such a model was presented in [10, 11] and has been employed to study the properties of plasma flows in the presence of a longitudinal field taking into account the finite conductivity of the medium. In addition, estimates of the efficiency of acceleration of a rotating plasma in the presence of a magnetic field have been obtained [11].

Verification of any numerical model involves its comparison with an analytical model and a comparison of the results obtained in calculations using various numerical models. The present paper considers a more complete two-fluid numerical MHD model, which is suitable in particular, for detailed studies of processes near the electrodes.

Modified MHD Equations. A two-fluid numerical model of two-dimensional flows and the results of the first numerical experiments in coaxial channels plasma accelerators in the presence of a longitudinal field are presented in [12]. The model is based on the MHD equations taking into account the Hall effect ($\boldsymbol{V}_e \neq \boldsymbol{V}_i$), the conductivity tensor of the medium and dependences of the transport coefficients in the magnetic field on the parameter $\omega_e\tau_e$ (ω_e is the electron cyclotron rotation frequency; τ_e is the time between electron–ion collisions) [13]. This model describes the ion current transport regime in which the plasma enters the channel, for example, through a transparent rod anode. In this case, according to the analytical model, some functions, in particular, the density $\rho(z)$ and azimuthal velocity $V_\varphi(z)$ are specified on the anode equipotential surface, which allows a comparison of analytical and numerical solutions. However, in this formulation of the problem, it is impossible to study the plasma dynamics for various parameters of the problem, including the longitudinal field.

The present paper considers a two-dimensional two-fluid numerical model for the plasma dynamics in an accelerator with ion current transport in the case of self-consistent plasma motion through the electrodes for various values of the longitudinal field and plasma parameters at the channel inlet. In the absence of a longitudinal field, the model with self-consistent plasma motion in the ion current transport regime has been used previously to study the processes in the accelerator channel with the traditional azimuthal component of the magnetic field H_φ [14]. For self-consistent plasma inflow in the presence of an additional longitudinal field ($H_\varphi \gg H_z \gg H_r$), it is also assumed that on the equipotential electrodes ($E_\tau = 0$ and $E_\varphi = 0$) there are no jumps and discontinuities of the quantities. [Here E_φ is the azimuthal component of the electric intensity and E_τ is the tangential component in the plane (z, r).]

Following [13], we consider the plasma quasineutral ($n_i = n_e = n$) and ignore the inertia of electrons ($m_e \ll m_i$). In the examined range of the problem parameters, standard estimates of the heat transfer and characteristic time of energy exchange between the components show that $T_i \simeq T_e = T$. In this paper, we will restrict ourselves to the dynamics of a hydrogen plasma ($Z = 1$ and $m = m_i = m_p$), often used in experiments.

Simple transformations of the initial transport equations using the magnetic field induction equation and the above assumptions yield the following system of equations [12]:

$$\frac{\partial\rho}{\partial t} + \operatorname{div}\rho\,\boldsymbol{V} = 0, \qquad \rho\,\frac{d\boldsymbol{V}}{dt} + \nabla P = \frac{1}{c}\,[\boldsymbol{j},\boldsymbol{H}],$$

$$\rho\,\frac{d\varepsilon}{dt} + P\operatorname{div}\boldsymbol{V} = Q - \operatorname{div}\boldsymbol{q} + \frac{k}{e(\gamma-1)}\,(\boldsymbol{j},\nabla)T + \frac{P_e}{e}\,\operatorname{div}\frac{\boldsymbol{j}}{n},$$

$$\frac{1}{c}\,\frac{\partial\boldsymbol{H}}{\partial t} = -\operatorname{rot}\boldsymbol{E}, \qquad \boldsymbol{E} = -\frac{1}{c}\,[\boldsymbol{V}_e,\boldsymbol{H}] - \frac{1}{en}\,\nabla P_e + \frac{1}{en}\,\boldsymbol{R}, \tag{1}$$

$$\boldsymbol{j} = \frac{c}{4\pi}\,\operatorname{rot}\boldsymbol{H} = en(\boldsymbol{V}_i - \boldsymbol{V}_e), \qquad \frac{d}{dt} = \frac{\partial}{\partial t} + (\boldsymbol{V},\nabla),$$

$$P = P_i + P_e = 2(c_p - c_v)\rho T, \qquad \varepsilon = 2c_v T, \qquad k/m = c_p - c_v = c_v(\gamma-1).$$

Here $\boldsymbol{V} = \boldsymbol{V}_i$, P is the total pressure, $\rho = mn$ is the heavy-particle density, $\boldsymbol{j}$ is the electric current, and $\boldsymbol{q}$ is the heat flux; the transport coefficients in the magnetic field depend on the parameter $\omega_e\tau_e$, where $\omega_e = eH/(m_e c)$ and $\tau_e = 3\sqrt{m_e}\,(kT)^{3/2}/(4\sqrt{2\pi}\,\lambda e^4 Z^2 n)$ (λ is the Coulomb logarithm).

The force of friction between the components of the medium $\boldsymbol{R} = \boldsymbol{R}_j + \boldsymbol{R}_T$ is the sum of the friction force $\boldsymbol{R}_j$ due to the presence of the relative velocity $\boldsymbol{u} = \boldsymbol{V}_e - \boldsymbol{V}_i = -\boldsymbol{j}/(en)$ and the thermal force $\boldsymbol{R}_T$ dependent on the temperature gradient. According to [13], we have

$$\boldsymbol{R}_j = \frac{en}{\sigma}\Big(A_1(x)\boldsymbol{j}_\parallel + A_2(x)\boldsymbol{j}_\perp - \frac{A_3(x)}{H}\,[\boldsymbol{H},\boldsymbol{j}]\Big),$$

$$\boldsymbol{R}_T = -kn\Big(B_1(x)\nabla_\parallel T + B_2(x)\nabla_\perp T + \frac{B_3(x)}{H}\,[\boldsymbol{H},\nabla T]\Big), \tag{2}$$

where $\boldsymbol{j}_\parallel = (\boldsymbol{j},\boldsymbol{H})\boldsymbol{H}/H^2$ and $\boldsymbol{j}_\perp = [\boldsymbol{H},[\boldsymbol{j},\boldsymbol{H}]]/H^2$ are the vector components parallel and perpendicular to the magnetic field; A_1, A_2, and A_3 and B_1, B_2, and B_3 are known functions of the variable quantity $x = \omega_e\tau_e$; $\sigma = e^2 n_e\tau_e/m_e$ is the electrical conductivity of the medium. The electron heat flux also consists of two flows: $\boldsymbol{q}_e = \boldsymbol{q}_j^e + \boldsymbol{q}_T^e$. The heat flux $\boldsymbol{q}_T^e$ due to the temperature gradient can be ignored since $q_T^e \ll q_j^e$. In addition, the ion heat flux is much smaller than the electron heat flux ($q_i \ll q_e$) and, hence it can also be ignored. Then,

$$\boldsymbol{q} = \boldsymbol{q}_e + \boldsymbol{q}_i \approx \boldsymbol{q}_j^e = -\frac{kT}{e}\Big(B_2(x)\boldsymbol{j} + \frac{B_1(x) - B_2(x)}{H^2}\,(\boldsymbol{j},\boldsymbol{H})\boldsymbol{H} + \frac{B_3(x)}{H}\,[\boldsymbol{H},\boldsymbol{j}]\Big).$$

The total heat release due to collisions is equal to

$$Q = Q_i + Q_e = (\boldsymbol{R},\boldsymbol{j})/(en).$$

Experimental studies (see, for example, [4, 5, 15]) and estimates of the parameters in the examined range indicate that using the ordinary transport coefficients is to some extent justified in numerical solutions not only of this problem but also a large number of other plasmadynamic problems (see, for example, [15, 16]).

Parameters of the Problem. Equations (1) and (2) are transformed and written in dimensionless form. As the normalizing quantities we use the following dimensional constants: the channel length L and the characteristic values of the concentration n_0 ($\rho_0 = mn_0$), temperature T_0, and azimuthal magnetic-field component at the channel inlet $H_0 = H_\varphi^0 = 2J_p/(cR_0)$ (R_0 is the radius of the outer electrode; J_p is the discharge current in the system). The pressure is normalized by the quantity $H_0^2/(4\pi)$, the characteristic velocity by $V_1 = H_0/\sqrt{4\pi\rho_0}$, time by $t_1 = L/V_1$, the electric field intensity by $E_1 = H_0V_1/c$, and the current density by the quantity $j_1 = cH_0/(4\pi L)$. The initial dimensional quantities are related to the dimensionless parameters used in the problem as follows: $\xi = (c/(eL))\sqrt{m/(4\pi n_0)}$ is the local exchange parameter characterizing the role of the Hall effect in the two-fluid regime; $\beta = 8\pi P_0/H_0^2$ is the ratio of the gas and magnetic pressures at the inlet ($P_0 = kn_0T_0$); $\nu = 1/\operatorname{Re}_m = c^2/(4\pi LV_1\sigma)$ is the magnetic viscosity which is inverse proportional to the magnetic Reynolds number corresponding to Spitzer conductivity. Using ξ and ν, we obtain $x = \omega_e\tau_e = \xi H/(\nu\rho)$.

In the plasma flow, the dimensionless conductivity depends on the temperature: $\operatorname{Re}_m = \sigma_0 T^{3/2}$; the parameter $\omega_e\tau_e$ can also have different values at different points of the channel. Using experimental data [4, 5] as the characteristic parameters of the problem we choose the following values: $n_0 = 3.6\cdot 10^{20}$ m^{-3}, $T_0 = 2$ eV, $J_p = 300$ kA, $L = 0.6$ m, and $R_0 = 0.25$ m. In this case, the values of the dimensionless parameters of the problem are $\beta = 0.005$, $\xi = 0.02$, $\sigma_0 = 812.8$. For $T = 1$ and $\rho = 1$, we have $\omega_e\tau_e = 16.2$ and $\nu = 0.0012$. In fact, the dimensionless parameters, along with the equations and boundary conditions, determine the plasma flow in the channel. It should be noted that, in modern plasma accelerators, $\beta \ll 1$; therefore, the temperature background has an insignificant effect on the plasma flow dynamics. Accordingly, the radiation transport is not a necessary element of this study and can be taken into account in the following.

Features of Numerical Model. In the numerical integration of the multidimensional MHD problem, it is assumed that the condition $\operatorname{div}\boldsymbol{H} = 0$ is satisfied. There are some approaches to providing solenoidality of the magnetic field. The simplest method is to write Eqs. (1) taking into account the vector potential $\boldsymbol{A}$ ($\boldsymbol{H} = \operatorname{rot}\boldsymbol{A}$). In cylindrical coordinates, we have

$$H_r = -\frac{\partial A_\varphi}{\partial z}, \qquad H_z = \frac{1}{r}\,\frac{\partial\,(rA_\varphi)}{\partial r}, \tag{3}$$

where A_φ is the azimuthal component of the vector potential $\boldsymbol{A}$. In the axisymmetric case, relations (3) provide exact satisfaction of the condition $\operatorname{div}\boldsymbol{H} = 0$, although in the momentum equations, it is necessary to approximate the second derivatives of the vector potential since

$$j_\varphi = \frac{\partial H_r}{\partial z} - \frac{\partial H_z}{\partial r} = -\Delta A_\varphi + \frac{A_\varphi}{r^2},$$

where

$$\Delta A_\varphi = \frac{\partial^2 A_\varphi}{\partial z^2} + \frac{1}{r}\frac{\partial}{\partial r}\Big(r\frac{\partial A_\varphi}{\partial r}\Big).$$

The results of numerical solution of the problem do not show considerable oscillations in the distribution of the second derivatives and rotations of the current due to the approximation of the derivatives.

In view of the aforesaid, Eqs. (1) and (2) for the axisymmetric case can be written in dimensionless form in terms of the components of the vector potential A_φ and the magnetic field component H_φ:

$$\frac{\partial \rho}{\partial t} + \frac{\partial(\rho V_z)}{\partial z} + \frac{1}{r}\frac{\partial(r\rho V_r)}{\partial r} = 0, \qquad \frac{\partial(\rho V_z)}{\partial t} + \frac{\partial}{\partial z}\Big(\rho V_z^2 + P + \frac{H_\varphi^2}{2}\Big) + \frac{1}{r}\frac{\partial(r\rho V_z V_r)}{\partial r} = j_\varphi \frac{\partial A_\varphi}{\partial z},$$

$$\frac{\partial(\rho V_r)}{\partial t} + \frac{\partial(\rho V_z V_r)}{\partial z} + \frac{1}{r}\frac{\partial}{\partial r}\Big[r\Big(\rho V_r^2 + P + \frac{H_\varphi^2}{2}\Big)\Big] = \frac{1}{r}\Big(\rho V_\varphi^2 + P - \frac{H_\varphi^2}{2}\Big) + \frac{j_\varphi}{r}\frac{\partial(rA_\varphi)}{\partial z},$$

$$\frac{\partial D_\varphi}{\partial t} + \frac{\partial(V_z D_\varphi)}{\partial z} + \frac{1}{r}\frac{\partial(rV_r D_\varphi)}{\partial r} = \frac{\partial(rA_\varphi)}{\partial r}\frac{\partial H_\varphi}{\partial z} - \frac{\partial A_\varphi}{\partial z}\frac{\partial(rH_\varphi)}{\partial r},$$

$$\frac{\partial(\rho\varepsilon)}{\partial t} + \frac{\partial(\rho\varepsilon V_z)}{\partial z} + \frac{1}{r}\frac{\partial(r\rho\varepsilon V_r)}{\partial r}$$

$$= -P\Big(\frac{\partial V_z}{\partial z} + \frac{1}{r}\frac{\partial(rV_r)}{\partial r}\Big) + \nu A_2(x)\Big[\Big(\frac{1}{r}\frac{\partial(rH_\varphi)}{\partial r}\Big)^2 + \Big(\frac{\partial H_\varphi}{\partial z}\Big)^2 + j_\varphi^2\Big] + Q_1 + Q_2,$$

$$\frac{\partial A_\varphi}{\partial t} + V_z\frac{\partial A_\varphi}{\partial z} + \frac{V_r}{r}\frac{\partial(rA_\varphi)}{\partial r} = \nu C_{\rm A}^\nu\Big(\Delta A_\varphi - \frac{A_\varphi}{r^2}\Big) - U_1\frac{\partial A_\varphi}{\partial z} + \frac{U_2}{r}\frac{\partial(rA_\varphi)}{\partial r},$$

$$\frac{\partial H_\varphi}{\partial t} + \frac{\partial(V_z H_\varphi)}{\partial z} + \frac{\partial(V_r H_\varphi)}{\partial r} = \frac{\partial(rA_\varphi)}{\partial r}\frac{\partial}{\partial z}\Big(\frac{V_\varphi}{r}\Big) - r\frac{\partial A_\varphi}{\partial z}\frac{\partial}{\partial r}\Big(\frac{V_\varphi}{r}\Big)$$

$$+ \frac{\partial}{\partial r}\Big(\nu\frac{C_r^\nu}{r}\frac{\partial(rH_\varphi)}{\partial r}\Big) + \frac{\partial}{\partial z}\Big(\nu C_z^\nu\frac{\partial H_\varphi}{\partial z}\Big) - 2\nu C_{rz}^\nu\frac{\partial^2(rH_\varphi)}{\partial r\,\partial z}$$

$$+ \frac{\partial(V_r^D H_\varphi)}{\partial r} + \frac{\partial(V_z^D H_\varphi)}{\partial z} + \frac{\partial F_1}{\partial z}\frac{\partial(rH_\varphi)}{\partial r} - \frac{\partial F_2}{\partial r}\frac{\partial(rH_\varphi)}{\partial z} - G_1\frac{\partial A_\varphi}{\partial z} + \frac{G_2}{r}\frac{\partial(rA_\varphi)}{\partial r} + \frac{\xi\beta}{2}W.$$

These equations contain the dimensionless variables $D_\varphi = r\rho V_\varphi$, $\varepsilon = \beta T/(\gamma-1)$, and $P = \beta\rho T$, the coefficients $C_{\rm A}^\nu = A_2 + (A_1 - A_2)H_\varphi^2/H^2$, $C_r^\nu = A_2 + (A_1 - A_2)H_z^2/H^2$, $C_z^\nu = A_2 + (A_1 - A_2)H_r^2/H^2$, and $C_{rz}^\nu = (A_1 - A_2)H_z H_r/H^2$, and the functions V_r^D, V_z^D, U_1, U_2, G_1, G_2, F_1, F_2, Q_1, Q_2, and W [12], which depend on the variables of the problems and are proportional to the parameters ξ, β, and ν much smaller than unity. Therefore, for smooth solutions, all terms containing the indicated functions can be treated as small additives that have little effect on the plasma dynamics as a whole. As a result, we have seven equations for the variables ρ, T, V_z, V_r, V_φ, H_φ, and A_φ.

For the given electrode profiles, the curvilinear computation domain in the variables (r, z) is mapped to a unit square $0 \leqslant y, z \leqslant 1$. In view of the Jacobian of the map, the initial unsteady MHD equations are written in the new variables in divergent form except for the equation for A_φ. The numerical solution of the problem is based on the coordinate split. The SHASTA-FCT algorithm with the phoenix correction for the hyperbolic part of the differential equations and the flow sweep method for the parabolic part describing diffusion along and across the magnetic field. The transport equation for the quantity A_φ is solved using a characteristic method. A more detailed description of the algorithms and references to the relevant literature are given in [12].

The numerical solution of the problem is performed until the establishment of flow. In the general unsteady, Eqs. (1) and (2) should be supplemented by the electric circuit equation. In this case, the calculation of the MHD problem is performed simultaneously with the calculation of current and voltage oscillograms. Such numerical experiments have been performed in the absence of a longitudinal field [7]. If the problem is solved using the circuit equation, then, for any time, a certain value of the circuit current corresponds to the solution of the MHD problem that coincides with the solution found using the relaxation method for the given current value. Use of this method is

also justified by the fact that the characteristic relaxation time is much smaller than the discharge time. Therefore, a qualitative analysis of the processes is based on obtaining quasi-steady-state solutions.

Boundary Conditions. At the channel inlet $z = 0$, the conditions of subsonic plasma flow with known distributions of the density $\rho(r) = f_1(r)$ and temperature $T(r) = f_2(r)$ are imposed. Specification of these functions according to the analytical model [9] provides verification of the solution. Ignoring the additional equation of the electric circuit, we can assume that the current has a constant value and enters the system only through the electrodes, i.e., $j_z = 0$ at $z = 0$ or $rH_\varphi = r_0 = \text{const}$, where $r_0 = R_0/L$. The plasma moves in a certain direction, for example, along the coordinate lines. We assume that, in the inlet section, the plasma does not rotate and the azimuthal velocity is equal to zero: $V_\varphi = 0$. At the inlet, we specify the longitudinal field $H_z \neq 0$. Following [9, 10], we have $H_z(r) = H_z^0 = \text{const}$. In view of (3), for $z = 0$ we obtain $A_\varphi = 0.5H_z^0 r$.

The channel geometry can be determined using analytical constructions [9] in the absence of a longitudinal field. The electrode shape corresponding to these constructions (Fig. 1) allows transonic flow to be implemented. In the central, narrowest, part of the channel, there is transition through the fast magnetosonic wave velocity; therefore, at the outlet for hypersonic flow, the free flow conditions are specified.

The boundary conditions on the electrodes $r_a(z)$ and $r_k(z)$ assumes their equipotentiality ($E_\tau = 0$ and $E_\varphi = 0$). These conditions allow one to determine the normal velocity component V_n [or V_r for the given geometry of the outer electrode $r_a(z) = r_0 = \text{const}$] that corresponds to the optimum delivery of the plasma through the electrodes. As shown by the calculations, the flow at the anode occurs in such a manner that $|V_r| \ll V_z$. In the presence of flow ($\rho V_n \neq 0$), the presumed absence of jumps of variables on the anode from a physical point of view implies the absence of rotational or Alfvén discontinuity on the anode equipotential surface.

Results of Calculations of Plasma Flows. Figure 1 gives an example of steady-state transonic plasma flow for the above characteristic parameters of the problem in the case where the longitudinal magnetic field at the inlet is equal to $H_z^0 = 0.1$. In this calculation version, the density at the inlet section varies under the law $\rho(0, r) = r_0^2/r^2$, according to the analytical model [9]. Assuming that the inflowing plasma is isentropic (entropy $s = c_v \ln P/\rho^\gamma = \text{const}$), at $z = 0$ we have $T = \rho^{\gamma-1}$. Figure 1 gives isolines $rH_\varphi = \text{const}$ which coincide with the electric field lines, the vector distribution of the magnetic field $\boldsymbol{H}$ in the plane (z, r), the azimuthal velocity of ions and electrons, the projection of the ion velocity onto the plane (z, r), and the density isolines ρ. In Fig. 1c, the scale of the vectors is determined by the scale of the characteristic velocity V_1.

In Fig. 1a (curve F), it is evident that, in the middle of the channel, the flow velocity passes through the local velocity of the fast magnetosonic wave

$$V_{fa}^2 = \frac{1}{2}\,(V_T^2 + V_\text{A}^2) + \frac{1}{2}\,\sqrt{(V_T^2 + V_\text{A}^2)^2 - 4V_T^2 V_\text{A}^2 \cos^2\theta}.$$

Here $V_T = \sqrt{\gamma P/\rho}$ is the thermal gas-dynamic sound velocity, $V_\text{A} = H/\sqrt{\rho}$, and $\cos\theta = (\boldsymbol{H}, \boldsymbol{V})/(HV)$. Curve A in Fig. 1b corresponds to transition through the Alfvén wave velocity $\boldsymbol{V}_\text{A} = \boldsymbol{H}/\sqrt{\rho}$. Both transitions occur smoothly and are not accompanied by discontinuities of MHD variables.

The distribution of the longitudinal magnetic field H_z has singularities (see Fig. 1a). As r increases, the quantity H_z increases and reaches the maximum value on the surface of the outer electrode in the central, narrowest, part of the accelerator channel: $H_z^\text{max} = H_z(z, r) = 0.5$ ($z \approx 0.5$, $r = r_0$). A similar value was obtained using the one-fluid model.

The azimuthal velocity $V_\varphi^{i,e}(z, r)$ (see Fig. 1b) increases in the radial and axial directions. In other words, the presence of a longitudinal field of small magnitude leads to plasma rotation, which, according to the one-fluid and analytical models, reaches the maximum value near the outer electrode at the exit from the accelerator channel: $V_\varphi^\text{max} = V_\varphi(z, r) = 0.72$ ($z = 1$, $r = r_0$). It should be noted that the difference in velocity between the ions and electrons (solid and dashed curves in Fig. 1b) is insignificant since, in the dimensionless variables, $\boldsymbol{V}_e = \boldsymbol{V}_i - (\xi/\rho)\boldsymbol{j}$ ($\xi \ll 1$). At the accelerator outlet $z = 1$, the kinetic energy due to rotation $\varepsilon_\varphi = \int\limits_{r_k}^{r_a} \rho V_\varphi^2 \pi r\, dr$, is a small part of the longitudinal kinetic energy of the outflowing flow $\varepsilon_z = \int\limits_{r_k}^{r_a} \rho V_z^2 \pi r\, dr$. In this case, $K_\varepsilon = \dfrac{\varepsilon_\varphi}{\varepsilon_z} \cdot 100\% = 14\%$. At the same time, in the calculations using the one-fluid model, $K_\varepsilon = 7\%$.

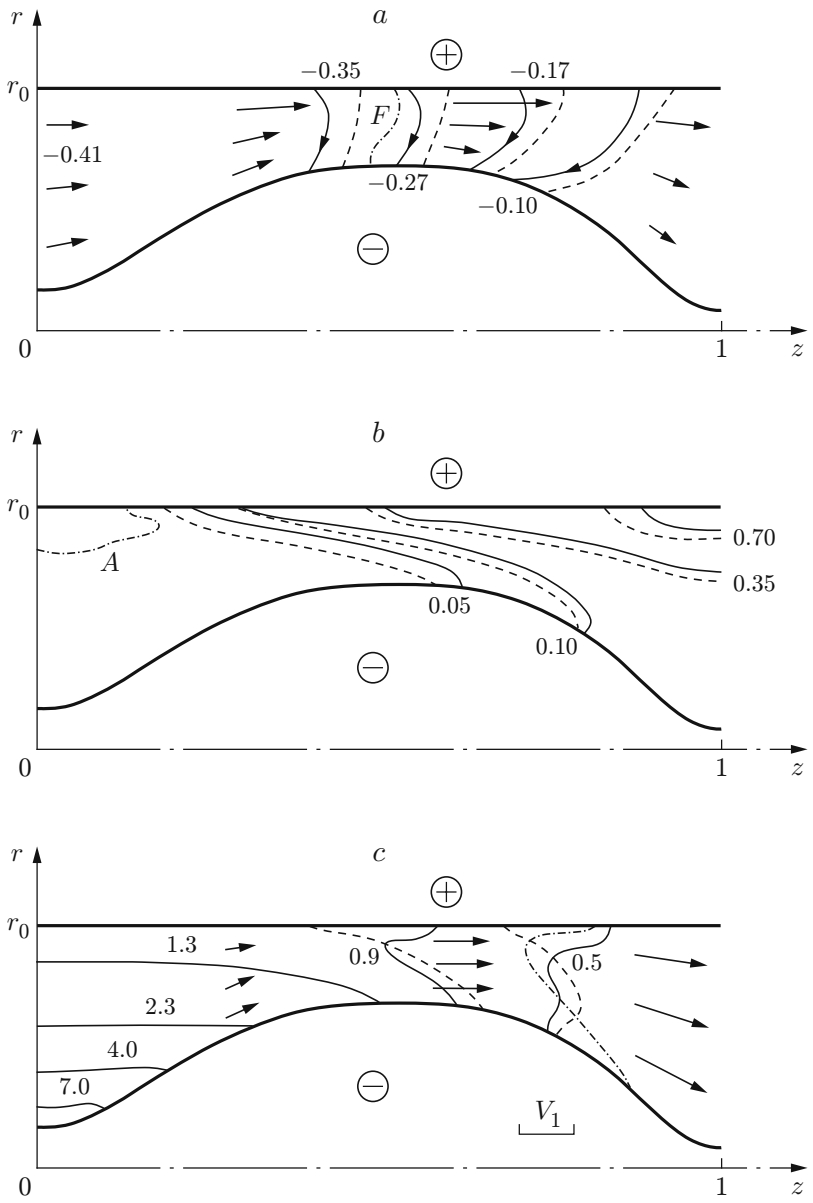

Fig. 1. Example of transonic plasma flow in the presence of a longitudinal magnetic field ($H_z^0 = 0.1$): (a) isolines of the function rH_φ (the solid curves correspond to the presence of a longitudinal magnetic field; the dashed curves to the absence of a longitudinal magnetic field); the dot-and-dashed curve F is the boundary of transition through the fast magnetosonic wave velocity; the arrows show the distribution of the magnetic field vector $\boldsymbol{H}$ in the plane (z, r); (b) azimuthal velocity (the solid curves correspond to ions; the dashed curves to electrons); the dot-and-dashed line A is the boundary of transition through the Alfén wave velocity; (c) density isolines ρ [in the presence of a longitudinal magnetic field (solid curves) and in the absence of a longitudinal magnetic field (dashed curves)]; the dot-and-dashed line correspond to the results of calculation for the analytical model; the arrows is the projection of the ion velocity onto the plane (z, r).

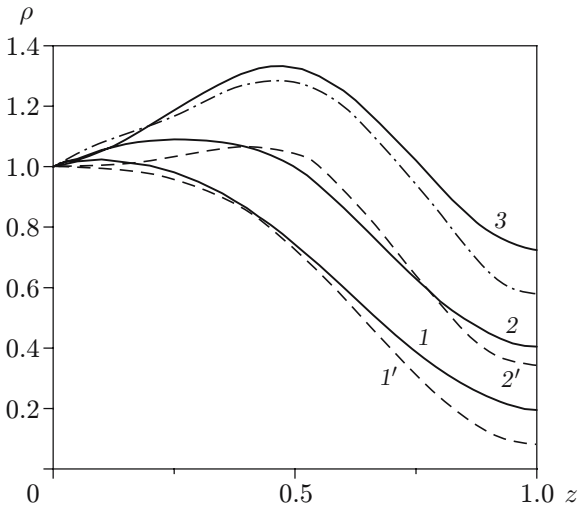

Fig. 2. Plasma density distribution along the outer electrode: curves 1, 2, and 3 correspond to the calculation for the two-fluid MHD model for $H_z^0 = 0$ (1), 0.1 (2), and 0.15 (3) and curves $1'$ and $2'$ correspond to the calculation for the analytical model for $H_z^0 = 0$ ($1'$) and 0.1 ($2'$); the dot-and-dashed curve corresponds to the calculation for the one-fluid model ($H_z^0 = 0.15$).

The density variation $\rho(z, r)$ (the solid curves in Fig. 1c) in the neighborhood of the outer electrode is due to the effect of the longitudinal magnetic field. In the presence of a magnetic field H_z near the outer electrode, the slope angle of the electric current Isolines changes (the solid and dashed curves in Fig. 1a for $H_z^0 = 0.1$ and 0, respectively). Simultaneously, in this region, there is a change of density distribution (solid and dashed curves in Fig. 1c). In the neighborhood of the outer electrode, there is an increase in the density due to the rotation of the plasma. Figure 2 gives curves of the density $\rho(z, r)$ ($r = r_0$) versus the coordinate z along the outer electrode for various values of H_z^0. The solid curves 1 and 2 correspond to the calculation results for $H_z^0 = 0$ and 0.1, respectively. At the exit from the accelerator ($z = 1$ and $r = r_0$), the density increases from the value ρ_1 in the absence of a longitudinal field to the value ρ_2 in the presence of the field. For $H_z^0 = 0.1$, the density increase coefficient in the presence of the longitudinal field, defined as the ratio $K_\rho = \rho_2/\rho_1$, is equal to 2.16, which is slightly larger than the result $K_\rho = 1.63$ predicted for the same parameters by the one-fluid model. According to the experiments in the absence of a field ($H_z^0 = 0$), in the neighborhood of the outer electrode (anode) closer to the exit there is a deficiency of ions due to the Hall effect. As a rule, this leads to a current crisis and prevents acceleration. Obviously, this problem can be solved (completely or partially) by introducing a small longitudinal field to the system, resulting in the rotation and pushing of the plasma to the outer electrode.

Further studies based on the complete two-fluid MHD model also confirm the other trends predicted within the framework of the one-fluid model. Increasing the longitudinal magnetic field leads to a density growth near the outer electrode. Curve 3 in Fig. 2 corresponds to the value $H_z^0 = 0.15$. Increasing the longitudinal field intensity leads to increases in the fraction of the energy of rotation and the density growth coefficient. In this case, $K_\varepsilon = 28\%$, $K_\rho = 3.8$, $H_z^{\max} = 0.8$, and $V_\varphi^{\max} = 0.86$. The values of K_ε and K_ρ obtained in the ion current transport regime are larger than the values $K_\varepsilon = 18\%$ and $K_\rho = 2.3$ calculated using the one-fluid model for $H_z^0 = 0.15$.

Let us compare the analytical solutions and calculation results of the steady-state flows obtained using the one-fluid model and the two-fluid model considered. These solutions should not coincide. Nevertheless, significant qualitative and quantitative differences between them are not observed (see Fig. 1c). In Fig. 2, the dashed curves $1'$ and $2'$ correspond to the calculation results for the analytical model for $H_z^0 = 0$ and 0.1, respectively, and the dot-and-dashed curve to the calculation results for the one-fluid model for $H_z^0 = 0.15$.

The two-fluid MHD model allows detailed studies of the plasma behavior near the electrodes, in particular, in the ion current transport regime considered. We recall that, in the one-fluid model, the Hall effect is ignored ($\boldsymbol{V}_e = \boldsymbol{V}_i$) and the boundary condition $V_n = 0$ implies that the plasma slides along the impermeable electrodes. An increase in the longitudinal field intensity in the system leads, along with an increase in the density, to a

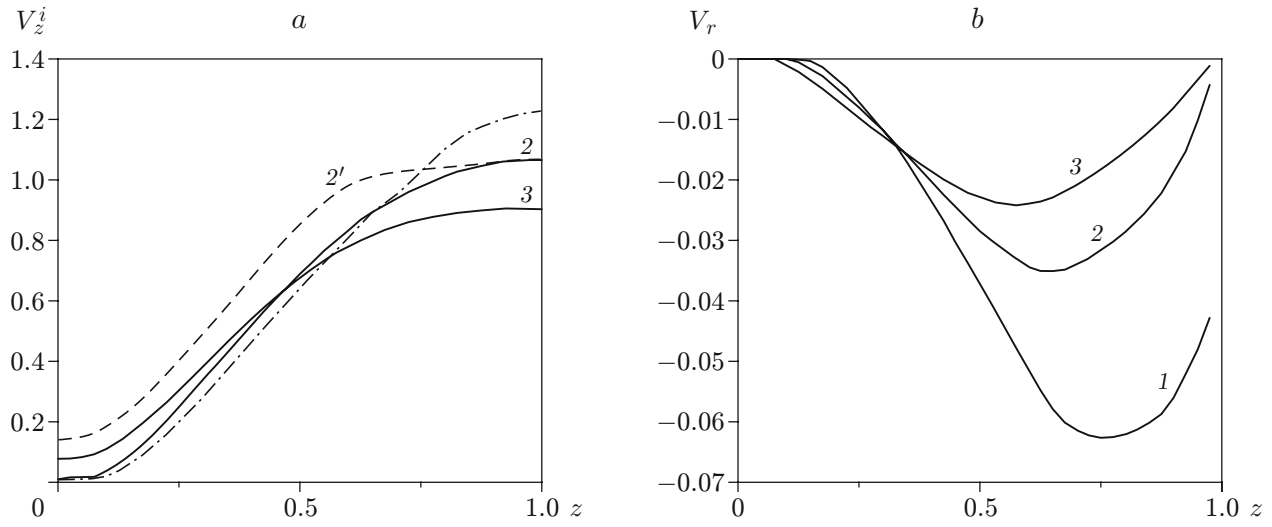

Fig. 3. Distribution of the longitudinal component (a) and radial component (b) of the plasma velocity along the outer electrode: the dot-and-dash curve shows the electron velocity calculated for the two-fluid MHD model; the remaining notation is the same as in Fig. 2.

slight decrease in the longitudinal component of the ion velocity V_z^i near the anode. In Fig. 3a, curves 2 and 3 correspond to the distributions of V_z^i along the anode for $H_z^0 = 0.10$ and 0.15, respectively, and curve $2'$ corresponds to the results of calculation for the analytical model for $H_z^0 = 0.1$. Using the two-fluid model, one can calculate the longitudinal components of the electron velocity $V_z^e = V_z^i - (\xi/\rho)j_z$. The dash-and-dotted curve in Fig. 3a corresponds to the distribution of V_z^e along the anode for $H_z^0 = 0.1$.

The following circumstance is of greater significance. The introduction of a longitudinal field to the system leads to both an increase in the density near the anode and a decrease in the normal or radial component V_r of the plasma inflow velocity (Fig. 3b). In this case, in the ion current transport regime with a longitudinal field, the integral plasma flow through the anode

$$\dot{m}_a = 2\pi r_0 \int_0^1 \rho V_r \, dz,$$

the flow through the cathode

$$\dot{m}_k = 2\pi \int_0^1 r_k(z) \rho V_n \, dz$$

and the integral exchange parameter $\xi_0 = |\dot{m}_a|/\dot{m}$ remain almost unchanged. Here the flow rate

$$\dot{m} = 2\pi \int_{r_k}^{r_a} r \rho V_z \, dr$$

can be determined from the channel inlet section $z = 0$. The calculations gave the integral parameters of the accelerator $\dot{m}_a$, $\dot{m}_k$, and ξ_0. In the dimensionless variables, $\dot{m}_a = -0.041$, $\dot{m}_k = -0.05$, and $\xi_0 = 0.27$ for $H_z^0 = 0$ and $\dot{m}_a = -0.039$, and $\dot{m}_k = -0.051$, $\xi_0 = 0.26$ for $H_z^0 = 0.1$. Thus, the presence of a longitudinal field does not lead to a significant change in the integral parameters of the accelerator, indicating that there is expedient to modify coaxial accelerators by using weak longitudinal magnetic fields, allowing changes in the plasma dynamics near the electrodes without considerably influencing the main flow.

Another purpose of the development of the two-fluid model was to confirm the qualitative flow rearrangement effect predicted by the one-fluid model for large values of the longitudinal field. Indeed, within the framework of the two-fluid model, the flow pattern changes beginning from a certain critical value of the longitudinal field, The

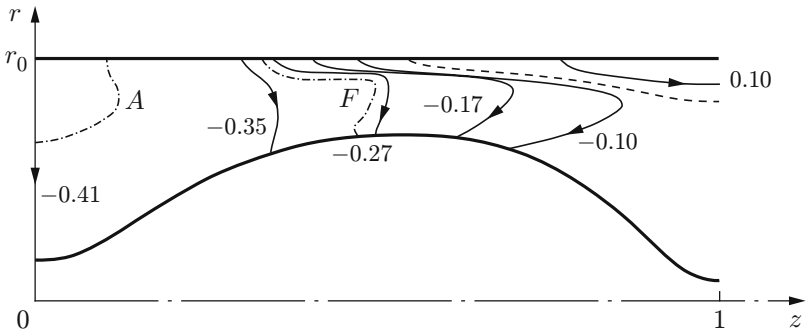

Fig. 4. Electric current isolines in plasma for $H_z^0 = 0.25$: the dashed curve corresponds to $H_\varphi = 0$; the dot-and-dashed curves A and F are the boundaries of transition through the Alfvén and fast magnetosonic wave velocities, respectively.

critical value of the field strength depends on the parameters of the problem and the plasma flow conditions at the inlet. Moreover, this value is approximately equal to the critical field intensity obtained in calculations for the one-fluid model. In the example considered in the present paper for $H_z^0 > 0.2$, near the outer electrode, where the longitudinal field has the maximum values, a narrow current layer and a region of almost uniform flow at a constant velocity are formed in the moving plasma. Outside, this region is bounded by the equipotential electrode, and within the channel, the region is separated from the main flow by the current layer (Fig. 4). This short-circuiting of the electric current on the external electrode suggests the possible attachment of the current (current concentration in a narrow zone at the plasma–conductor interface) in the case of large values of H_z^0. In comparison with the one-fluid model there is an inappreciable increase in the angle between the anode and current layer. The calculations for the analytical model [9] also gave the critical intensity of the longitudinal field. For values $H_z^0 > 0.15$, the analytical solution corresponding to the transonic plasma flow was not found.

In addition, the two-fluid model was used to calculate numerical experiments in the case of uniform plasma flow at the inlet ($\rho = 1$ and $T = 1$ at $z = 0$). The calculation results confirmed the main trends revealed for nonuniform flow and agree with the results calculations for the one-fluid model [10]. Variations in the parameters of the problem such as T_0 and J_p do not lead to significant changes in the processes described above. As the values of T_0 and J_p increase, the critical field intensity decreases slightly. In contrast, for a denser plasma (for example, $n_0 = 3.6 \cdot 10^{21}$ m^{-3}), the range of the longitudinal field $H_z^0 < 0.4$ corresponding to laminar flow, is extended. However, large values of the longitudinal field are of no interest. In this case, the fraction of the energy due to rotation is high.

Conclusions. The numerical experiments performed using the two-dimensional two-fluid MHD model showed that a small longitudinal magnetic field provided transonic plasma flows in the coaxial accelerator channel under various conditions of plasma flow at the inlet. At the exit from the accelerator, the fraction of the energy due to rotation is much lower than the kinetic energy of the longitudinal plasma flow.

It was established that a weak longitudinal magnetic field acting along the entire length of the channel leads to a gradual increase in the velocity of plasma rotation. As a result, the plasma concentration near the outer electrode increases. The increase in the density near the anode indicates the possibility of overcoming or reducing the current crisis in plasma accelerators. At the same time, for large values of the longitudinal field, one observed the formation of current layer in the moving plasma and current attachments at the outer electrode, in agreement with the previously developed one-fluid model.

Characteristic features of flow dynamics near the anode were found under conditions of optimum supply and self-consistent flow of the plasma through permeable equipotential electrodes in the ion current transport regime. The maximum values in the plasma flow distribution through the anode are reached in the central, narrowest, part of the channel. Integral plasma flows through the electrode surfaces and the integral exchange parameter are slightly affected by the magnitude of the longitudinal field.

This work was supported by the Russian Foundation for Basic Research (Grant No. 06-02-16707).

REFERENCES

1. A. I. Morozov, *Introduction to Plasma Dynamics* [in Russian], Fizmatlit, Moscow (2006).
2. V. E. Fortov (ed.), *Encyclopedia of Low-Temperature Plasma* [in Russian], Vol. 3, Nauka, Moscow (2000), p. 407.
3. A. I. Morozov, "Principles of coaxial (quasi) steady-state plasma accelerators (QSPAs)," *Fiz. Plazmy*, **16**, No. 2, 131–146 (1990).
4. V. G. Belan, S. P. Zolotarev, V. F. Levashov, et al., "Experimental study of a quasi-steady-state plasma accelerator powered from inductive and capacitive storages," *Fiz. Plazmy*, **16**, No. 2, 176–185 (1990).
5. V. I. Tereshin, A. N. Bandura, O. V. Byrka, et al., "Application of powerful quasi-steady-state plasma accelerators for simulation of ITER transient heat loads on divertor surfaces," *Plasma Phys. Control. Fusion*, **49**, A231–A239 (2007).
6. K. V. Brushlinskii, A. M. Zaborov, A. N. Kozlov, et al., "Numerical simulation of plasma flows in QSPA," *Fiz. Plazmy*, **16**, No. 2, 147–157 (1990).
7. A. N. Kozlov, "Plasma dynamics in QSPA during flow establishment," *Fiz. Plazmy*, **18**, No. 6, 714–723 (1992).
8. A. N. Kozlov "Kinetics of ionization and recombination in the channel of a plasma accelerator," *Izv. Ross. Akad. Nauk, Mekh. Zhidk. Gaza*, No. 5, 181–188 (2000).
9. A. N. Kozlov, "Effect of a longitudinal magnetic field on the Hall effect in the channel of a plasma accelerator," *Izv. Ross. Akad. Nauk, Mekh. Zhidk. Gaza*, No. 4, 165–175 (2003).
10. A. N. Kozlov, "Dynamics of rotating flows in the channel of a plasma accelerator with a longitudinal magnetic field," *Fiz. Plazmy*, **32**, No. 5, 413–422 (2006).
11. A. N. Kozlov, "Basis of the quasi-steady plasma accelerator theory in the presence of a longitudinal magnetic field," *J. Plasma. Phys.*, **74**, No. 2, 261–286 (2008).
12. A. N. Kozlov "Numerical model of rotating axisymmetric plasma flows. Comparison with the analytical model," Preprint No. 48, Keldysh Institute of Applied Mathematics, Moscow (2004).
13. S. I. Braginskii, "Transport phenomena in plasma," in: M. A. Leontovich (ed.), *Issues of Plasma Theory* (collected scientific papers) [in Russian], No. 1, Gosatomizdat, Moscow (1963), pp. 183–272.
14. K. V. Brushlinskii, A. N. Kozlov, and A. I. Morozov, "Numerical study of two-dimensional plasma flows and ionizing gas using the method of trial particles," *Fiz. Plazmy*, **11**, No. 11, 1358–1367 (1985).
15. V. T. Astrelin, A. V. Burdakov, and V. V. Postupaev, "Inhibition of thermal conduction and generation of ionic-sound waves during plasma heating by an electronic beam," *Fiz. Plazmy*, **24**, No. 5, 450–462 (1998).
16. A. A. Barmin and V. S. Uspenskii "Study of the nonsteady propagation of an ionizing shock wave in a magnetic field," *J. Appl. Mech. Tech. Phys.*, **3**, 356–362 (1989).